Polymerization of *rac*-Lactide Using Schiff Base Aluminum Catalysts: Structure, Activity, and Stereoselectivity

Hongzhi Du,[†,‡] Xuan Pang,[†,‡] Haiyang Yu,[†] Xiuli Zhuang,[†] Xuesi Chen,*[,†,‡] Dongmei Cui,[†,‡] Xianhong Wang,[†,‡] and Xiabin Jing[†,‡]

State Key Laboratory of Polymer Physics and Chemistry, Changchun Institute of Applied Chemistry, Chinese Academy of Sciences, Changchun 130022, China, and Graduate School, Chinese Academy of Sciences, Beijing 100039, China

Received September 21, 2006; Revised Manuscript Received January 6, 2007

ABSTRACT: A series of aluminum ethyls and isopropoxides based upon N,N,O,O-tetradentate Schiff base ligand framework have been prepared. X-ray diffraction analysis and ^{1}H NMR confirmed that these Schiff base aluminum ethyls and isopropoxides were all monomeric species with a five-coordinated central aluminum in their solid structures. Compared to the aluminum ethyls which all retain their monomeric structure in the solution, the dinucleating phenomenons of aluminum isopropoxides with less steric hindered substituents in the solution have also been observed. The activities and stereoselectivities of these complexes toward the ring-opening polymerization of *rac*-lactide have been investigated. Polymerization experiments indicated that (SB-**2d**)AlO^{i}Pr [(SB-**2d**) = 2,2-dimethyl-1,3-propylenebis(3,5-di-*tert*-butylsalicylideneiminato)] exhibited the highest stereoselectivity and (SB-**3b**)AlO^{i}Pr [(SB-**3b**) = 2,2-dimethyl-1,3-propylenebis(3,5-dichlorinesalicylideneiminato)] possessed the highest activity among these aluminum isopropoxides. The substituents and the mode of the bridging part between the two nitrogen atoms both exerted significant influences upon the progress of the polymerizations, influencing either the tacticity of isolated polymers or the rate of polymerization. The polymerization kinetics using (SB-**3b**)AlO^{i}Pr as a catalyst were studied in details, and the experimental results revealed that the rate of polymerization was first-order in [LA] and 1.81th-order with respect to (SB-**3b**)AlO^{i}Pr, which indicated that the propagating species was not uniform in the system without the protection of steric hindered substituents. Furthermore, the polymerization by initiating with (SB-**3b**)AlO^{i}Pr could be progressed at low temperatures (0 °C) without the change of stereoselectivity.

Introduction

Biodegradable polymers have recently attracted much interest and are considered to be excellent replacements for conventional oil-based materials. Among those most promising candidates in the class of materials, poly(lactic acid)s (PLAs) derived from totally renewable resources such as corn or sugar beets have many unique biodegradable and biocompatible properties superior to those of traditional olefin-based polymers. Therefore, they may have many environmental, biomedical, and pharmaceutical applications.[1] Although several methods for the synthesis of PLAs exist, the most convenient route is the ring-opening polymerization (ROP) of lactide, which is a cyclic dimer of lactic acid, catalyzed by various metal catalysts, such as tin,[2] zinc,[3] ferrous,[4] aluminum,[5] yttrium,[6] and titanium.[7] Stereochemistry plays an important role in the microstructures of PLAs, determining the mechanical properties, biodegradability, and ultimately the end use of this material. Emphasis has been put on the design and synthesis of well-defined metal complexes function as efficient and selective lactide polymerization catalysts during these years. Recent advances have resulted in a variety of PLA architectures being derived from either the racemic mixture or *meso*-lactide.[8] Systematic studies have demonstrated that the auxiliary ligand surrounding might significantly influence polymerization behavior of those catalysts.

Among the variety of catalysts, many chiral aluminum alkoxides supported by tetradentate Schiff base ligands prepared from salicylaldehyde have been identified to be notable as highly selective for the polymerization of *rac*-lactide or *meso*-lactide (Figure 1). Spassky et al.[9] discovered that ((*R*)-SalBinap)-AlOMe could give a highly stereocontrolled polymerization of *rac*-LA, to form isotactic and crystalline PLA with a higher T_m than optically pure PLLA. Coates et al.[10] reported *rac*-(SalBinap)AlO^{i}Pr could yield predominantly isotactic PLAs with T_m of 179−191 °C. Feijen et al.[11] succeeded in the polymerization of highly crystalline PLAs that had long isotactic sequences with a T_m of 183.5 °C using *rac*-cyclohexylsalen aluminum isopropoxides in solution and bulk polymerization.

Although these chiral Schiff base aluminum catalysts polymerize *rac*-LA in a well-stereocontrolled manner, the cost of these chiral catalysts is very high. Fortunately, achiral Schiff base aluminum alkoxides also possess the same stereocontrolled ability. Nomura[12a] has synthesized a series of achiral Schiff base aluminum ethyls and studied their polymerization behaviors. He suggested that the more flexible propylene backbone could give rise to a much higher stereoselectivity than catalysts with ethylene backbone. Nomura[12b] and us[13] have also reported that achiral (SB-**2d**)AlEt could afford poly(*rac*-LA) with a P_m of 90% and a high T_m of 201 °C[14] in the presence of 2-propanol. To expand upon our initial work, we were interested in investigating the effect of catalyst architectures on lactide polymerization behaviors, such as stereoselectivity and activity. Herein, we report a series of achiral Schiff base aluminum isopropoxides generated by in situ alcoholysis of aluminum ethyls for the polymerization of *rac*-lactide.

* Corresponding author. E-mail: xschen@ciac.jl.cn.
† Changchun Institute of Applied Chemistry.
‡ Graduate School.

10.1021/ma062194u CCC: $37.00
Published on Web 02/16/2007

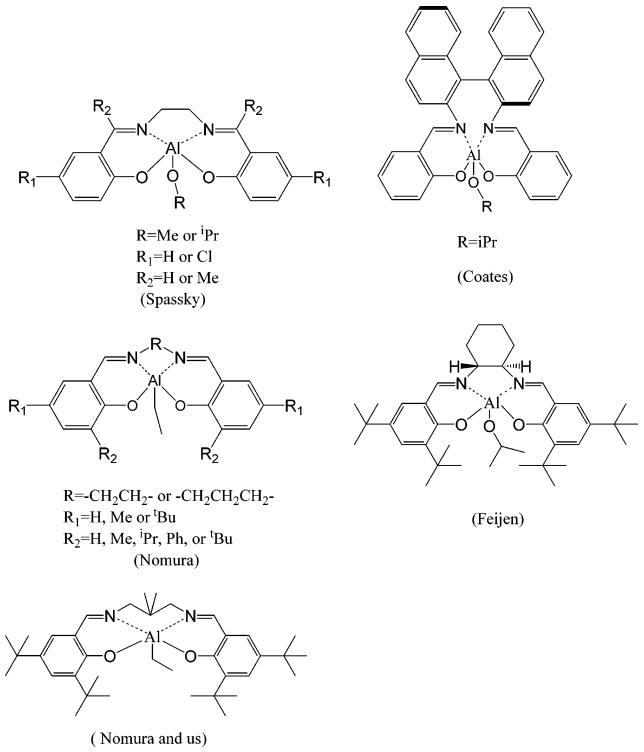

Figure 1. Schiff base aluminum catalysts explored for stereoselective ROP of *rac*-LA.

Results and Discussion

Synthesis and Determination of Structures in Solid State. The Schiff base aluminum ethyls (Figure 2) were prepared by treatment of the appropriate ligands with stoichiometric $AlEt_3$ in toluene at 70 °C (Scheme 1). All these complexes were isolated as solids in quantitative yields. X-ray diffraction analysis of the crystals of (SB-**2a**)AlEt,[15a] (SB-**2f**)AlEt, (SB-**3a**)AlEt, (SB-**1d**)AlEt, (SB-**2d**)AlEt,[15b] and (SB-**3b**)AlEt grown from concentrated toluene solution revealed analogous monomeric structures with two distinct geometries of central aluminum atoms. The geometry of five-coordinated aluminum atom can be classified into square pyramidal (sqp) and trigonal bipyramidal (tbp) measured by τ value ranges from 0 (for ideal sqp) to 1 (for ideal tbp) (Scheme 2).[16] (SB-**2a**)AlEt, (SB-**2f**)AlEt, and (SB-**3a**)AlEt with two carbon atoms backbone exhibit more sqp geometries with τ values of 0.44, 0.48, and 0.17, respectively. It is apparent that by introducing the bulky *tert*-butyl group on the phenol rings the geometries of central aluminum in (SB-**2a**)AlEt and (SB-**2f**)AlEt become more distorted than (SB-**3a**)AlEt. The molecular structure of (SB-**2f**)AlEt (Figure 3) depicts a sqp geometry with the ethyl group lying on the axial position and two nitrogen atoms and two oxygen atoms on the basal position. The aluminum atom is ca. 0.565 Å above the N(1)N(2)O(1)O(2) mean plane with a compressed axial O(1)−Al−N(2) bond angle of 158.80(9)° and equatorial N(1)−Al−C(35), N(1)−Al−O(2), and C(35)−Al−O(2) bond angles of 115.31(10)°, 129.73(9)°, and 114.35(10)°. The distances between the Al atom and O(1), O(2), N(1), N(2), and C(35) are 1.8320(17), 1.7903(16), 2.013(2), 2.066(2), and 1.974(3) Å. The structure of (SB-**3a**)AlEt (Figure 4) is an analogue of (SB-**2f**)AlEt with the average compressed axial N(1)−Al−O(2) bond angle of 152.50(7)° and equatorial N(2)−Al−C(17), N(2)−Al−O(1), and C(17)−Al−O(1) bond angle of 105.13(8)°, 142.24(7)°, and 111.80(8)°. The distances from the Al atom to O(1), O(2), N(1), N(2), and C(17) are 1.8144(15), 1.8268(15), 2.0472(18), 2.0129(18), and 1.974(2) Å. However, because of the backbone of three carbon atoms, the geometries of central aluminum atoms in (SB-**1d**)AlEt, (SB-**2d**)AlEt, and (SB-**3b**)AlEt are tbp with τ values of 0.88, 0.76, and 0.82. The molecular structure of (SB-**1d**)AlEt (Figure 5) exhibits a tbp geometry with N(2), O(1) atoms occupying the axial site and N(1), O(2), and the ethyl group lying on the equatorial plane. The aluminum atom lays ca. 0.094 Å above the equatorial plane formed by C(20), N(1), and O(2) in the direction of O(1). The average compressed axial N(2)−Al−O(1) bond angle is 170.53(8)°, and the equatorial O(2)−Al−N(1), O(2)−Al−C(20), and C(20)−Al−N(1) bond angles are 117.47(8)°, 118.77(11)°, and 122.05(11)°, very close to a typical tbp geometry. The distances from the aluminum atom to O(1), O(2), N(1), N(2), and C(20) are 1.8302(16), 1.7887(17), 1.998(2), 2.080(2), and 1.980(3) Å. The molecular structure of (SB-**3b**)AlEt (Figure 6) is an analogue of (SB-**1d**)AlEt. The sqp and tbp geometries deviation among these Schiff base aluminum ethyls indicate that the modification of the bridging part in the ligand leads to a dramatic change in the coordination geometry of the metal center, which is consistent with the previous observation.[17]

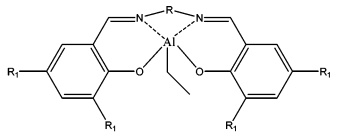

Cat.	R	R_1	Cat.	R	R_1
1a	$(CH_2)_2$	H	2a	$(CH_2)_2$	tBu
1b	$(CH_2)_3$	H	2b	$(CH_2)_3$	tBu
1c	$(CH_2)_4$	H	2c	$(CH_2)_4$	tBu
1d	$CH_2C(CH_3)_2CH_2$	H	2d	$CH_2C(CH_3)_2CH_2$	tBu
1e	o-$C_6H_3CH_2$	H	2e	o-$C_6H_3CH_2$	tBu
3a	$(CH_2)_2$	Cl	2f	$(CH_3)_2CCH_2$	tBu
3b	$CH_2C(CH_3)_2CH_2$	Cl	2g	o-C_6H_4	tBu

Figure 2. Schiff base aluminum ethyls prepared in this paper.

To better mimic and investigate the structures of the actual initiating species in the solid and solution state, Schiff base aluminum isopropoxides (SB-**1d**)AlO^{i}Pr, (SB-**2d**)AlO^{i}Pr,[18] and (SB-**3b**)AlO^{i}Pr were prepared by in situ alcoholysis. Treatment of the three appropriate aluminum ethyls with stoichiometric 2-propanol in toluene or treatment of the Schiff base ligands directly with Al(O^{i}Pr)$_3$ both resulted in the formation of the three desired aluminum isopropoxides along with the release of C_2H_6 or 2-propanol (Scheme 1). X-ray diffraction analysis had previously revealed the molecular structure of (SB-**2d**)AlO^{i}Pr to be a monomeric species with a distorted tbp geometry. X-ray diffraction analysis of crystal of (SB-**3b**)AlO^{i}Pr (Figure 7) grown from toluene revealed a similar monomeric structure, with no significant perturbations of the central core. For example, the bond lengths of the Al−O [1.820 Å] and Al−N [2.031 Å] on the axial site of (SB-**3b**)AlO^{i}Pr are extremely the same as Al−O [1.818 Å] and Al−N [2.030 Å] in (SB-**2d**)AlO^{i}Pr, while the other bond lengths in the core are only slightly different from each other. Moreover, comparison of the bond angles in the central core of (SB-**3b**)AlO^{i}Pr with (SB-**3b**)AlEt reveals that the axial average compressed angle O(1)−Al(1)−N(2) of (SB-**3b**)AlO^{i}Pr is 172.2(2)°, larger than 168.33(11)° of (SB-**3b**)AlEt, and the largest equatorial angle of (SB-**3b**)AlO^{i}Pr is N(1)−Al(1)−O(2) which is 118.2(2)°, less than 118.99(13)° of (SB-**3b**)AlEt. It is well indicated that (SB-**3b**)AlO^{i}Pr with a τ value of 0.85 possesses a more typical tbp geometry

Scheme 1. Synthesis of Schiff Base Aluminum Ethyls and Isopropoxides

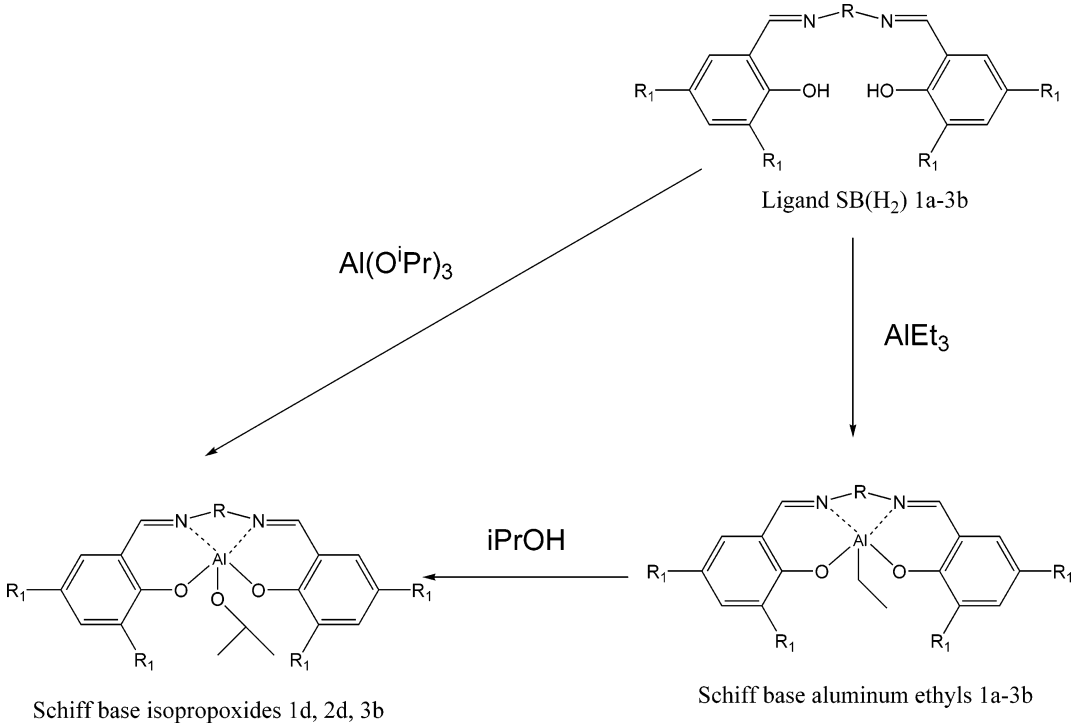

Scheme 2. Two Different Geometries of Five-Coordinate Central Aluminum Atom

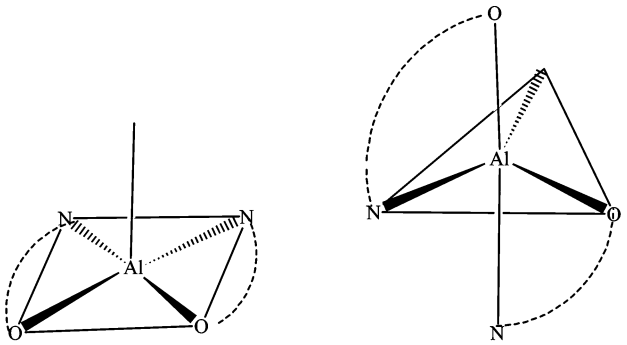

than its ethyl counterpart (SB-**3b**)AlEt with a τ value of 0.78. The molecular structure of (SB-**1d**)AlO^{i}Pr (Figure 8) as determined by X-ray diffraction is also a monomeric species with a τ value of 0.82. It is reasoned that the Schiff base aluminum isopropoxides, even without the protection of bulky *tert*-butyl groups, all adopt monomeric species in their solid states due to the large steric hindered effect caused by the secondary isopropoxide groups, which is consistent with the previous observation by Coates.[10a]

Determination of Structures in Solution. The ^{27}Al NMR spectra of all the aluminum ethyls revealed them to retain their monomeric structures with five-coordinated central aluminum in solution with single peaks exhibited at about 30−35 ppm.[19] Aluminum isopropoxide (SB-**2d**)AlO^{i}Pr was previously observed to be monomeric in the chloroform-d_1 solution, in agreement with the monomeric structure in its solid state. However, (SB-**1d**)AlO^{i}Pr had a complex ^{1}H NMR spectrum with two sets of resonance peaks (Figure 9). The resonance peaks of the four protons of $-CH_2-$ groups on the backbone may help distinguish the two different species. Because the monomeric species could not retain its chiralty due to the fast exchange between the two conformational stereoisomers in the NMR time scale, the two major doublets appeared at 3.93 and 3.13 ppm are ascribed to the four bridge protons in the monomeric species. The four minor doublets appeared at 4.78, 3.53, 3.31, and 2.77 ppm were also ascribed to the bridge protons, which indicated another species to be rigid and nontautomerized in the solution. The only probable reason for the disappearance of tautomerization phenomenon for this species is the formation of dimeric structure by an Al_2O_2 core in the solution state.[20] The existence of equilibrium between monomeric and dimeric species was also confirmed by the appearance of two singlet at 34.37 and 3.75 ppm in the ^{27}Al NMR spectrum of (SB-**1d**)AlO^{i}Pr. The monomeric species holded ca. 70.6% according to the integrals in the ^{1}H NMR spectrum at room temperature. Although (SB-**1d**)AlO^{i}Pr possesses very poor solubility in common deuterated solvents such as d_8-toluene and d_4-dichlorobenzene for VT NMR, a preliminary study on this equilibrium was conducted in $CDCl_3$ within a narrow temperature range from 25 to 60 °C. At 40 °C, the monomeric species accounts for ca. 74.2% in the medium solution; however, this proportion increased to ca. 79.5% at 60 °C. According to Gibbs free energy equation, the activation parameters for this transformation of dimeric species to monomeric species

$$\text{dimeric species} \rightleftharpoons \text{monomeric species}$$

are calculated as follows: $\Delta H^{\ddagger} = +17.63$ kcal mol^{-1} and $\Delta S^{\ddagger} = +110.74$ cal mol^{-1} K^{-1}. We concluded that the monomeric species might dimerize in the solution medium due to the solvent effect, while the positive activation entropy was the driving force of this tranformation to monomeric species which dominated in the medium under polymerization conditions. The ^{1}H NMR spectrum of (SB-**3b**)AlO^{i}Pr revealed a completely dimeric structure with two different signals for the two imine protons and four different doublets for the four protons of $-CH_2-$ on the bridge. This dimeric structure was further confirmed by the apperance of a singlet at 2.14 ppm in the ^{27}Al NMR spectrum. It is well concluded that without the presence of steric hindered *tert*-butyl substituent on the phenolate rings the monomeric species of these Schiff base aluminum isopropoxides may

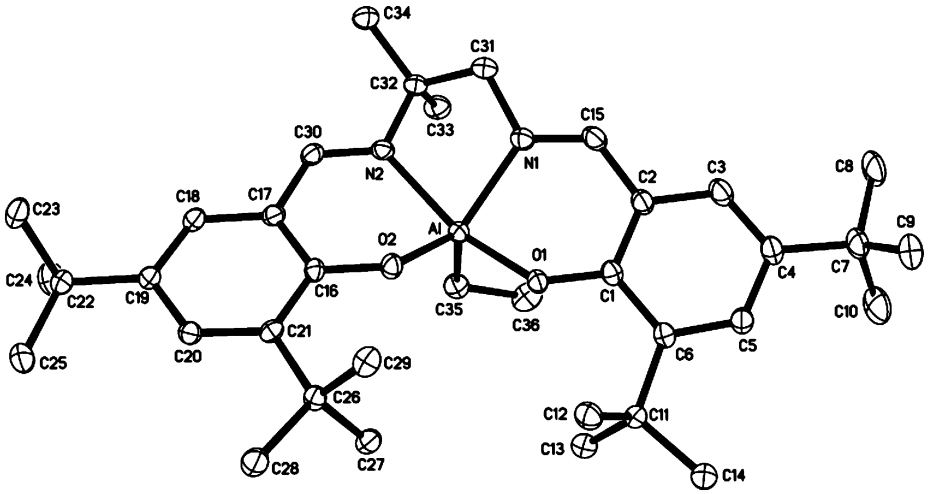

Figure 3. X-ray structure of (SB-**2f**)AlEt, with all non-hydrogen atoms shown as 30% thermal ellipsoids. CCDC: 291531.

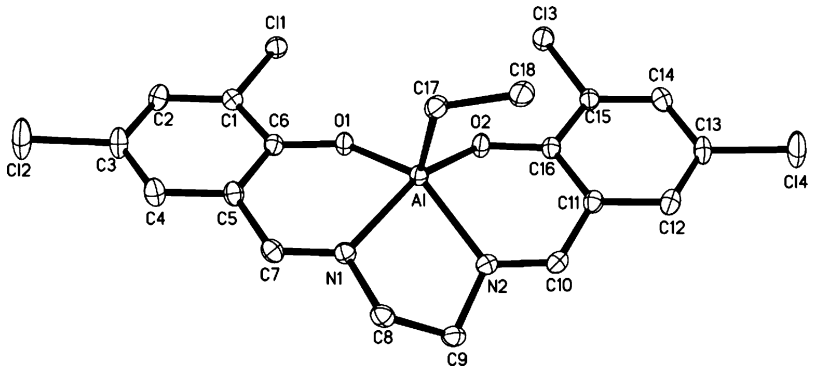

Figure 4. X-ray structure of (SB-**3a**)AlEt, with all non-hydrogen atoms shown as 30% thermal ellipsoids. CCDC: 298665.

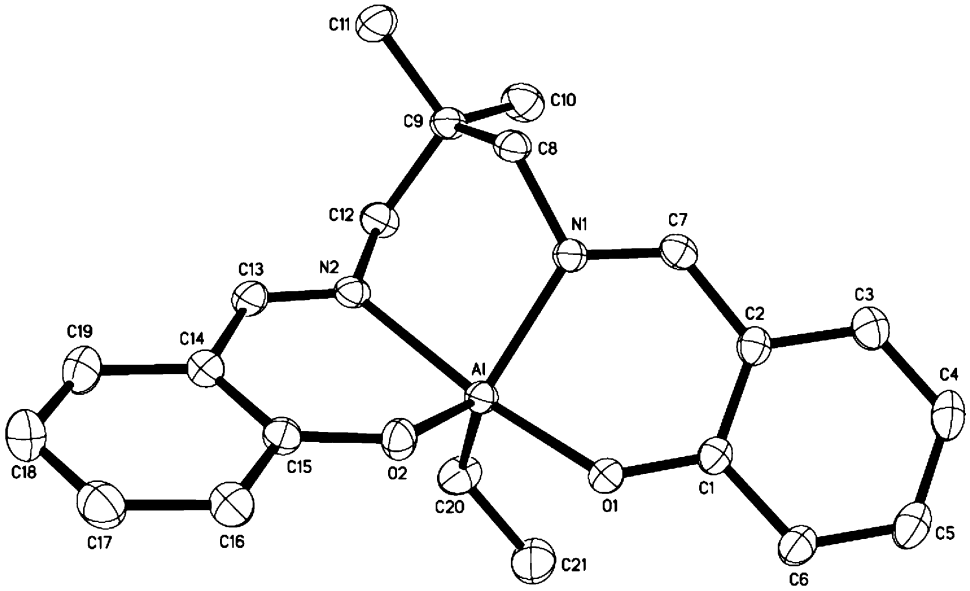

Figure 5. X-ray structure of (SB-**1d**)AlEt, with all non-hydrogen atoms shown as 30% thermal ellipsoids. CCDC: 292364.

dimerize in the solution state, and the electron-withdrawing substituents at the ortho and para positions on the phenolate rings facilitate this dimerization due to electronical effects.

Mechanism and Kinetics of *rac*-Lactide Polymerization. The ^{1}H NMR spectrum of oligomer prepared using (SB-**2a**)-AlEt at a low concentration ratio of monomer to catalyst is shown in Figure S1 in the Supporting Information. The two doublets combined to be a triplet at 1.24 ppm (**a**) and the quartet at 4.34 ppm (**f**), with an integral ratio close to 6:1, were assigned to the methyl protons of the isopropoxycarbonyl end group and the methine proton neighboring the hydroxyl end group. These features suggest that the two end groups of this poly(*rac*-LA) are isopropoxycarbonyl and hydroxyl group and may further confirm that the ROPs follow the coordinative-insertion mechanism.[21]

The presence of the substituent ortho to the phenolic hydroxy group plays an important role in determining the rate of polymerization. The introduction of bulky *tert*-butyl substituents

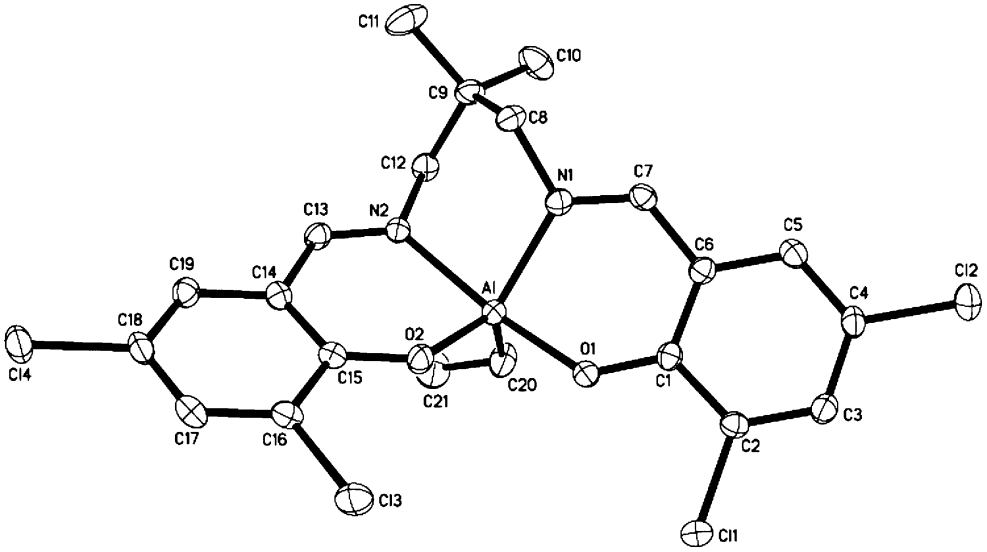

Figure 6. X-ray structure of (SB-**3b**)AlEt, with all non-hydrogen atoms shown as 30% thermal ellipsoids. CCDC: 292527.

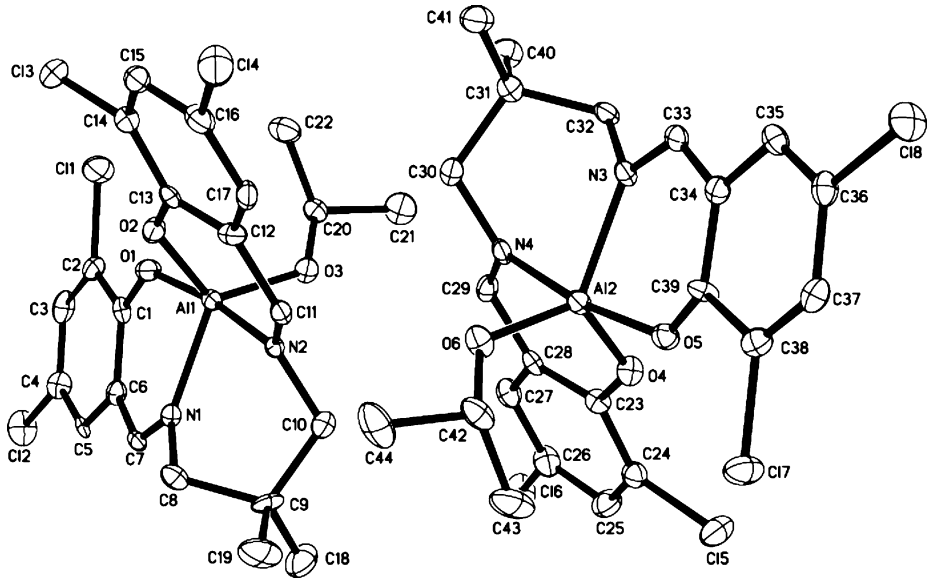

Figure 7. X-ray structure of (SB-**3b**)AlO^{i}Pr, with all non-hydrogen atoms shown as 30% thermal ellipsoids. CCDC: 295900.

at the ortho position generally brings the effect of protecting the active species and slowing down the polymerization rate. The *p*-phenolate substituent was commonly varied to provide the catalyst different electron-donating ability, but its function on polymerization rate was demonstrated to be complex.[22] (SB-**3b**)AlO^{i}Pr with chlorine atoms at both ortho and para positions was confirmed to possess the highest polymerization activity among all the Schiff base aluminum isopropoxides we studied. Polymerization experiments revealed that the *rac*-lactide polymerization initiated with (SB-**3b**)AlO^{i}Pr reached 96.3% conversion within 3 h, exhibiting a much faster polymerization rate than those initiated with (SB-**1d**)AlO^{i}Pr of 96.3% conversion within 22 h and (SB-**2d**)AlO^{i}Pr of 95.4% conversion within 9 h. The high activity of (SB-**3b**)AlO^{i}Pr could also be confirmed by the polymerization of *rac*-lactide at low temperatures (Table 2). The conversions of *rac*-lactide could reach 95.3% and 41.9% after 48 h at 40 and 0 °C, respectively, without significant decrease in selectivity (entries 4 and 5, Table 2). It is also indicated that the bridging part between the two nitrogen atoms also influences the polymerization rate. The comparison between (SB-**2e**)AlEt (k_{app} = 2.10 × 10^{-3} min^{-1}) and (SB-**2b**)AlEt (k_{app} = 1.17 × 10^{-3} min^{-1}) (Figure 10) revealed that the formation of highly conjugated structure resulting from the presence of a benzene ring on the backbone could accelerate the polymerization progress. Moreover, the introduction of gem-alkyl substituents on the backbone also enhances the activities of catalysts, which were compared by (SB-**2b**)AlEt (k_{app} = 1.17 × 10^{-3} min^{-1}) and (SB-**2d**)AlO^{i}Pr (k_{app} = 7.28 × 10^{-3} min^{-1}) as well as (SB-**2a**)AlEt (reached 15.6% conversion after 72 h) and (SB-**2f**)AlEt (reached 28.3% conversion after 72 h) (Table 1).

Our previous study demonstrated that (SB-**2d**)AlO^{i}Pr polymerized *rac*-lactide in a first-order kinetic manner in both monomer and catalyst[18] (Figure 11a). In order to fully understand the nature of *rac*-lactide polymerization using catalysts with less steric substituent, the conversions of *rac*-lactide with time at various concentrations of (SB-**3b**)AlO^{i}Pr in toluene at 70 °C were monitored by ^{1}H NMR spectroscopy until the monomer consumption was achieved ($[LA]_0$ = 0.53 mol L^{-1}: $[LA]_0/[Al]$ = 120, 88, and 69; $[LA]_0$ = 0.20 mol L^{-1}: $[LA]_0/[Al]$ = 100; $[LA]_0$ = 0.10 mol L^{-1}: $[LA]_0/[Al]$ = 60). In each case, an induction period and first-order kinetics in monomer were observed to obtain the semilogarithmic plots for these polymerizations, as shown in Figure 12. Thus, the polymeri-

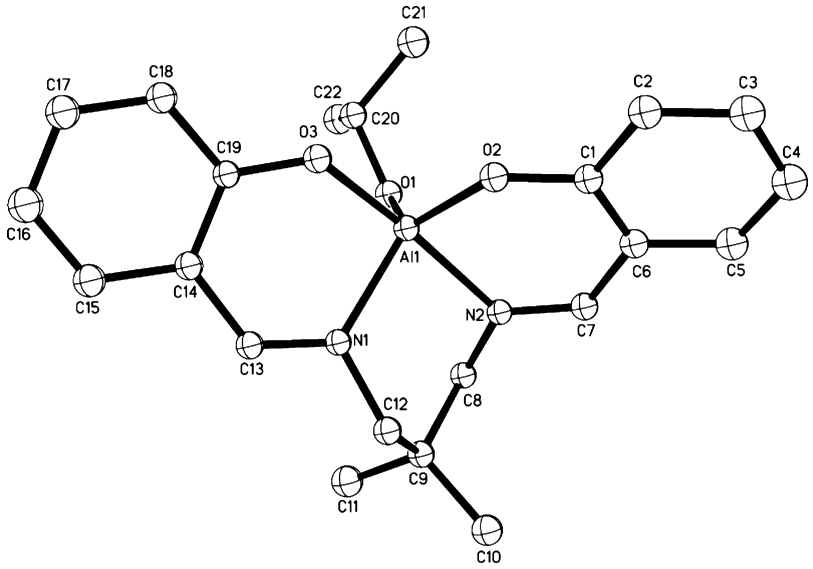

Figure 8. X-ray structure of (SB-**1d**)AlO^{i}Pr, with all non-hydrogen atoms shown as 30% thermal ellipsoids. CCDC: 617430.

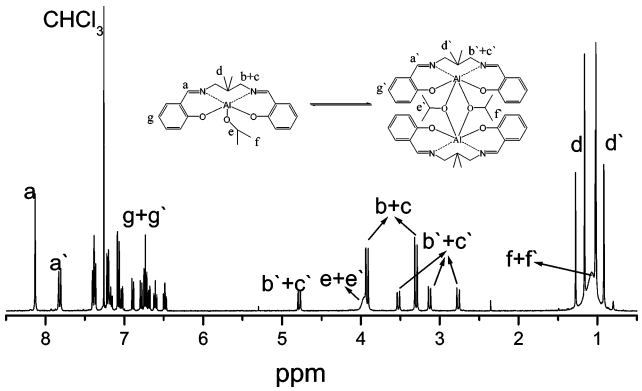

Figure 9. ^{1}H NMR spectrum of (SB-**1d**)AlO^{i}Pr in $CDCl_3$ solution at 25 °C.

zation of *rac*-lactide by (SB-**3b**)AlO^{i}Pr presumably proceeds according to

$$-\mathrm{d[LA]}/\mathrm{d}t = k_{app}[\mathrm{LA}] \quad (1)$$

where $k_{app} = k_p[\mathrm{Al}]^x$, and k_p is the propagation rate constant. To determine the order in aluminum (x), ln k_{app} is plotted vs ln $[\mathrm{Al}]_0$ (Figure 11b). From this plot, the order in catalyst which can be shown by the plot slope is 1.81. Therefore, the polymerization of *rac*-lactide by (SB-**3b**)AlO^{i}Pr follows the following overall kinetic law:

$$-\mathrm{d[LA]}/\mathrm{d}t = k_p[\mathrm{Al}]^{1.81}[\mathrm{LA}] \quad (2)$$

Fractional dependencies upon catalysts have been previously reported for several cases of lactone ring-opening polymerization with zinc,[23a,b] ferrous,[23c] and stannous[23d] alkoxides. Such noninteger orders in catalyst are difficult to interpret mechanistically, but it is commonly believed to result from the reversible balance between nonaggregate and aggregrate species in the polymerization medium.[24] Although it cannot be fully determined whether the dimeric species of catalysts possess polymerization activity, the kinetic order related to catalyst concentration is above 1, which does indicate that the propagation of the aggregated species is faster than the nonaggragated form. Comparison of the kinetic order in catalyst between (SB-**2d**)-AlO^{i}Pr and (SB-**3b**)AlO^{i}Pr indicates that the bulky substituents ortho to the phenolic hydroxy group protect the active species to be nonaggregate and thus form the singular species in the polymerization system. It is also postulated that the singularity of active species accounts for the high selectivities of catalysts and low PDI of the resultant polymers.

The parameter "efficiency" is defined as the percentage of active initiators, calculated from the observed M_n relative to the theoretical ones, assuming that each aluminum atom of active species initiates one polymer chain. Most of the efficiencies of the Schiff base aluminum initiators in Table 1 are approximately equal to 1.0, indicating the molecular weights determined by gel permeation chromatography (GPC) analysis correlate well with the monomer conversion and, thus, reflecting the nature of living and controlled polymerization catalyzed by these initiators. The efficiencies of (SB-**1e**)AlEt and (SB-**2f**)AlEt were 1.47 and 1.48, respectively, much higher than 1.0, which suggested a significant transesterification reaction during the polymerization process. The initiators (SB-**3a**)AlEt and (SB-**3b**)AlEt bearing chlorine atoms on their phenolate rings possessed much lower efficiencies, having a value of 0.56 and 0.70, which probably suggested that, under the polymerization conditions studied, there existed an equilibrium between the monomeric and dimeric initiator species.

Stereochemistry of *rac*-Lactide Polymerization. All the polymerizations were carried out in toluene at 70 °C, using Schiff base aluminum isopropoxide catalysts generated by in situ alcoholysis of Schiff base aluminum ethyl complexes. Since all the Schiff base ligands prepared here were achiral, it is anticipated that these catalysts might be capable of stereochemical control in the polymerization of *rac*-lactide via a predominated chain-end control mechanism.[12a,23b,25] Under Bernoullian statistics, successive additions of different enantiomeric monomers are independent events, so the rates of addition of L- and D-monomers to the growing chain ends are not affected by the configuration of the last repeating unit. Atatic poly(*rac*-LA)s are most probably prepared under this condition. Because there was a preference for isotactic addition during the ROPs of *rac*-LA in our research, the intensity values of the individual stereosequences did not obey Bernoullian statistics, and a Markovian process should be used to interpret the stereosequence distribution instead.[26] According to the first-order Markovian statistics,[27] PLA derived from *rac*-lactide can exhibit up to five tetrad sequences, which are *mmm*, *mmr*, *rmm*, *mrm*,

Table 1. Stereoselective Polymerization of *rac*-LA with Discrete Schiff Base Aluminum Catalysts[a]

	cat.	M/I	time (h)	conv (%)[b]	$M_{n,Cal}$[c] × 10^{-3}	$M_{n,GPC}$[d] × 10^{-3}	PDI[d]	efficiency[e]	P_m[f] (%)	T_m (°C)
1	**1a**	58.2	22	85.3	7.36	10.56	1.22	1.20	71	n.a.
2	**1b**	60.7	9	95.5	8.53	15.66	1.53	0.94	67	n.a.
3	**1c**	62.0	9	85.9	7.74	13.48	1.10	0.99	71	n.a.
4	**1d**	58.9	22	96.3	8.24	13.51	1.38	1.05	67	n.a.
5	**1e**	61.1	9	90.6	8.18	9.59	1.12	1.47	69	n.a.
6	**2a**	62.2	72	15.6	1.46	2.40	1.09	1.05	82	165.6
7	**2b**	59.4	9	41.0	3.57	6.96	1.06	0.89	86	182.5
8	**2c**	60.5	48	66.6	5.87	9.76	1.09	1.04	69	158.1
9	**2d**	57.4	9	95.4	7.95	13.05	1.09	1.05	90	191.0
10	**2e**	69.8	12	61.6	6.26	10.58	1.08	1.02	82	175.5
11	**2f**	56.1	72	28.3	2.35	2.73	1.08	1.48	72	142.2
12	**2g**	55.0	240	65.3	5.38	9.97	1.08	0.93	62	n.a.
13	**3a**	57.2	14	94.3	7.83	24.3	1.49	0.56	70	n.a.
14	**3b**	58.1	3	96.3	8.27	20.23	1.36	0.70	71	n.a.

[a] All polymerizations were carried out in toluene solution at 70 °C, $[LA]_0 = 0.53$ mol L^{-1}. [b] Measured by ^1H NMR. [c] Calculated from the equation $M_{n,Cal}$ = (M/I) × conversion × 144.13 + 60. [d] Determined by GPC in THF, relative to PS standard. The true value of M_n could be calculated according to formula $M_n = 0.58M_{n,GPC}$.[31] [e] Efficiency is defined as the percentage of active initiators, calculated from the observed M_n relative to the theoretical ones, assuming that each aluminum atom of active species initiates one polymer chain. [f] The parameter P_m is the tetrad probabilities of poly(*rac*-LA) are $[mmm] = P_m^2 + (1 - P_m)P_m/2$, $[mmr] = [rmm] = (1 - P_m)P_m$, $[rmr] = (1 - P_m)$,[2] and $[mrm] = [(1 - P_m)^2 + P_m(1 - P_m)]/2$.

Table 2. Stereoselective Polymerization of *rac*-LA with (SB-3b)AlO^{i}Pr at Different Temperatures[a]

entry	M/I	T (°C)	time (h)	conv[b] (%)	$M_{n,GPC}$[c]	PDI[c]	P_m[d] (%)
1	378	110	1	83.5	45.5	1.20	71
2	180	90	1	85.3	21.8	1.11	69
3	58	70	3	96.3	12.4	1.20	71
4	75	40	48	95.3	11.9	1.09	71
5	75	0	48	41.9	4.74	1.05	70

[a] All polymerizations were carried out at a $[LA]_0$ of 0.53 mol L^{-1}; entries 1−3 were carried out in toluene solution while entries 4 and 5 were carried out in dichloromethane solution. [b] Measured by ^1H NMR. [c] Determined by GPC in THF, relative to PS standard. The true value of M_n could be calculated according to the formula $M_n = 0.58M_{n,GPC}$.[31] [d] The parameter P_m is the tetrad probabilities of poly(*rac*-LA) are $[mmm] = P_m^2 + (1 - P_m)P_m/2$, $[mmr] = [rmm] = (1 - P_m)P_m$, $[rmr] = (1 - P_m)^2$, and $[mrm] = [(1 - P_m)^2 + P_m(1 - P_m)]/2$.

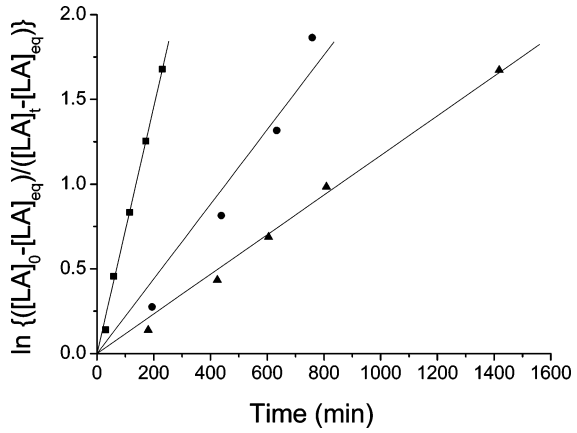

Figure 10. Kinetics of the ROP of *rac*-LA by discrete initiators in toluene at 70 °C with $[M]_0 = 0.52$ mol L^{-1}, $[LA]_{eq} = 0.046$ mol L^{-1}, $[Al]_0$:[^{i}PrOH]$_0$ = 1:1, $[Al]_0 = 8.67 \times 10^{-3}$ mol L^{-1}: (●) initiator (SB-**2e**)AlO^{i}Pr, $k_{app} = 2.10 \times 10^{-3}$ min^{-1}; (▲) initiator (SB-**2b**)AlO^{i}Pr, $k_{app} = 1.17 \times 10^{-3}$ min^{-1}; (■) initiator (SB-**2d**)AlO^{i}Pr, $k_{app} = 7.28 \times 10^{-3}$ min^{-1}.

and *rmr*, in its ^1H NMR spectrum in relative ratios determined by the ability of the catalyst to control racemic [*r*-diad] and meso [*m*-diad] connectivity of the monomer units. Determination of the stereochemical microstructures of PLA is achieved through inspection of the methine region of homonuclear decoupled ^1H NMR spectra of the resultant polymers.[28] Microstructural analysis of PLA formed from *rac*-lactide reveals that all these complexes have the abilities to influence on the tacticity of the polymer chains, and this ability varies according to their different auxiliary ligand surroundings.

(SB-**2d**)AlO^{i}Pr was previously demonstrated to be a highly selective catalyst which afforded substantially isotactic PLA with a P_m of 0.90. Upon heating the reaction mixture to 110 and 130 °C, P_m can be diminished to 0.82 and 0.77, respectively. According to first-order Markovian statistics, the probability for *meso* linkages could be determined as[29]

$$P_m = k_m/(k_m + k_r) = k_{S/SS}(k_{S/SS} + k_{S/RR}) = k_{R/RR}/(k_{R/RR} + k_{R/SS}) \quad (3)$$

where $k_{S/SS}$ and $k_{S/RR}$ are the propagation rates of adding another LLA/DLA monomer to a living chain ending with a S lactic acid unit and $k_{R/RR}$ and $k_{R/SS}$ represent the propagation rate of adding another DLA/LLA monomer to a living chain ending with a R lactic acid unit. According to absolute reaction rate theory, we could obtain the following equations:

$$P_m = k_m/(k_m + k_r) = k_{S/SS}/(k_{S/SS} + k_{S/RR})$$
$$P_m = k_m/(k_m + k_r) = k_{R/RR}/(k_{R/SS} + k_{R/RR}) \quad (4)$$

$$k_{S/SS} = k_{R/RR} = k_m = (KT/h)\exp[(\Delta S_m^{\ddagger}/R) - (\Delta H_m^{\ddagger}/RT)]$$
$$k_{S/RR} = k_{R/SS} = k_r = (KT/h)\exp[(\Delta S_r^{\ddagger}/R) - (\Delta H_r^{\ddagger}/RT)] \quad (5)$$

In order to determine the activation entropy and enthalpy difference between the competition formation of isotactic and syndiotactic stereosequences, eq 6 could be deduced from the above equations:

$$\frac{P_m}{1 - P_m} = \frac{k_m}{k_r} = \exp[(\Delta S_m^{\ddagger} - \Delta S_r^{\ddagger})/R - (\Delta H_m^{\ddagger} - \Delta H_r^{\ddagger})/RT] \quad (6)$$

Figure 13 could be drawn through plotting ln $[P_m/(1 - P_m)]$ against $10^3/T$. The slope of the plot is in direct proportion to the enthalpy difference while the intercept is in proportion to

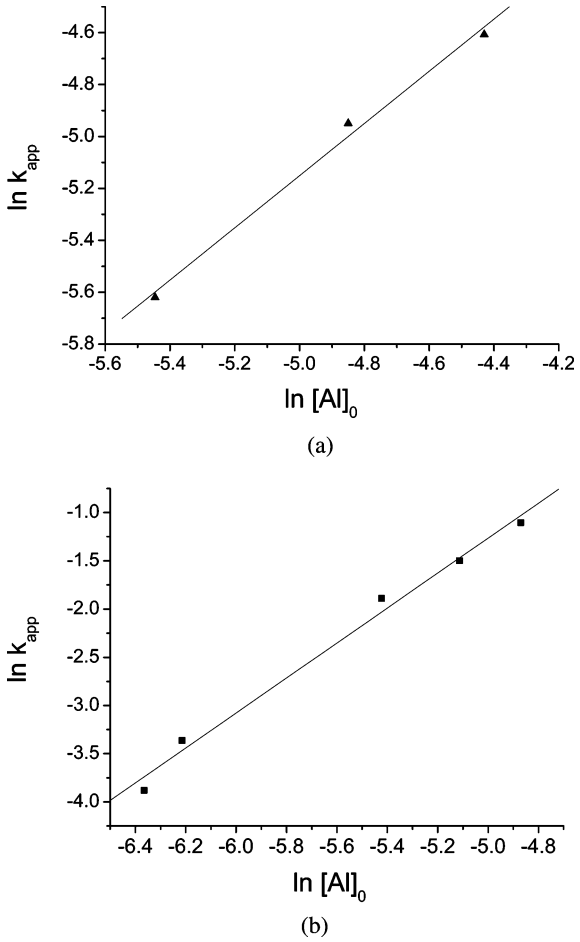

Figure 11. (a) Plot of ln k_{app} vs ln $[Al]_0$ for the polymerization of *rac*-lactide with (SB-**2d**)AlO^{i}Pr as catalyst (toluene, 70 °C, $[LA]_0$ = 0.53 mol L^{-1}). (b) Plot of ln k_{app} vs ln $[Al]_0$ for the polymerization of *rac*-lactide with (SB-**3b**)AlO^{i}Pr as catalyst (toluene, 70 °C).

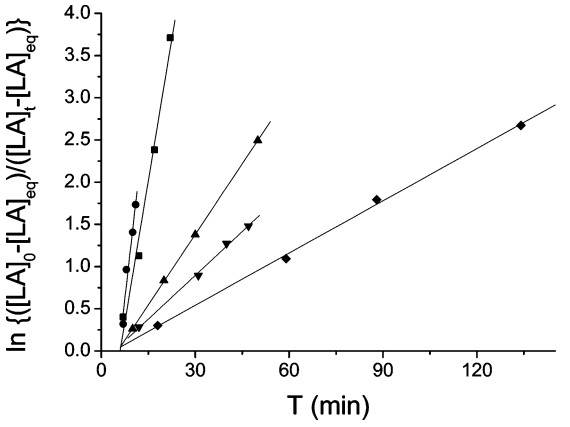

Figure 12. Semilogarithmic plots of *rac*-lactide conversion with time in toluene at 70 °C with (SB-**3b**)AlO^{i}Pr as catalyst ($[LA]_0$ = 0.53 mol L^{-1}: ●, [LA]/[Al] = 69; ■, [LA]/[Al] = 88; ▲, [LA]/[Al] = 120; $[LA]_0$ = 0.20 mol L^{-1}: ▼, [LA]/[Al] = 100; $[LA]_0$ = 0.10 mol L^{-1}: ◆, [LA]/[Al] = 60).

the entropy difference. While the analysis presented above revealed an activation entropy difference ($\Delta S_m^{\ddagger} - \Delta S_r^{\ddagger}$) of -18.0 ± 2.5 cal/(K mol) and activation enthalpy difference ($\Delta H_m^{\ddagger} - \Delta H_r^{\ddagger}$) of -12.2 ± 0.9 kcal/(K mol), which explained the preference of isotactic stereosequence by using (SB-**2d**)-AlEt. Similarly, analysis of the microstructures of the resulting poly(*rac*-LA)s prepared by using (SB-**1e**)AlEt revealed ($\Delta S_m^{\ddagger}$

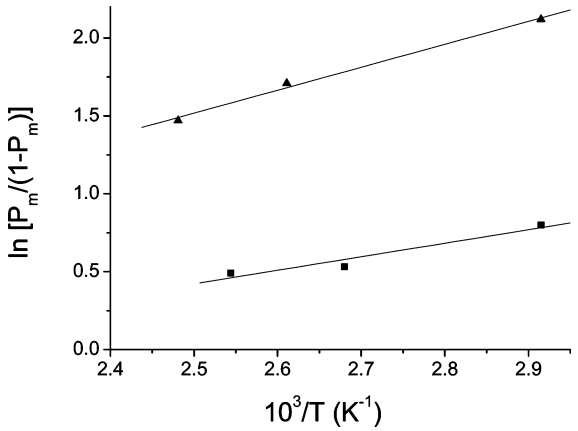

Figure 13. Relationship between polymerization temperatures and stereochemistries of resulting poly(*rac*-LA)s by using (SB-**2d**)AlEt (▲) and (SB-**1e**)AlEt (■), respectively.

$- \Delta S_r^{\ddagger}$) and ($\Delta H_m^{\ddagger} - \Delta H_r^{\ddagger}$) were of -14.6 ± 4.9 cal/(K mol) and -7.23 ± 1.8 kcal/(K mol), respectively (Figure 13).

Furthermore, the polymerization data indicated that the substituents at the ortho positions on the phenol rings of Schiff base ligand significantly affect the ability of the catalysts to control monomer insertion. For instance, changing the *tert*-butyl substituents in (SB-**2d**)AlEt (P_m = 0.90) to hydrogen atoms in (SB-**1d**)AlEt resulted in a dramatic decrease in isotacticity (P_m = 0.67). Similarly, this trend can also be shown from the comparison between (SB-**2a**)AlEt (P_m = 0.82) and (SB-**1a**)-AlEt (P_m = 0.71), (SB-**2b**)AlEt (P_m = 0.86) and (SB-**1b**)AlEt (P_m = 0.67), and (SB-**2e**)AlEt (P_m = 0.82) and (SB-**1e**)AlEt (P_m = 0.69). The origins for this dramatic change in selectivities are consistent with the previous observations that the enhancement of stereoselectivity requires bulky substituents at the ortho positions for the stereoselective polymerization adopting chain-end control mechanism.[12a,23b,25] In such a reaction, the bulky substituents not only favor mononuclear complex formation to limit chain aggregation during the polymerization process but also increase the influence of the stereogenic center of the last inserted monomer, which in turn determines the microsequence of stereocenters on the polymer chain.

The modification of the bridging part in the ligand also led to significant change in selectivities of these catalysts. It is apparent that PLA prepared with (SB-**2g**)AlEt (P_m = 0.62) is less isotactic than that prepared with (SB-**2a**)AlEt (P_m = 0.82), possibly due to the enhancement of conjugated molecular structure resulting from the benzene rings on the backbone to form rigid planar geometry. Comparison between (SB-**2e**)AlEt (P_m = 0.82) and (SB-**2b**)AlEt (P_m = 0.86) is also consistent with this lack of tacticity. (SB-**2b**)AlEt with three carbon atom backbone was found to have higher stereoselectivity (P_m = 0.86) compared to (SB-**2a**)AlEt (P_m = 0.82) with two carbon atom backbone and (SB-**2c**)AlEt (P_m = 0.69) with four carbon atom backbone. However, without *tert*-butyl groups, (SB-**1b**)AlEt with three carbon atom backbone possessed a poorer stereoselectivity (P_m = 0.67) than (SB-**1a**)AlEt (P_m = 0.71) with two carbon atom backbone and (SB-**1c**)AlEt (P_m = 0.71) with four carbon atom backbone. The introduction of gem-alkyl groups onto the backbone also revealed a distinguished effect on stereoselectivity. (SB-**2f**)AlEt with gem-alkyl groups on the two carbon atom bridge afforded less isotactic PLA (P_m = 0.72) compared to that polymerized using (SB-**2a**)AlEt (P_m = 0.82) without gem-alkyl groups. Nevertheless, (SB-**2d**)AlEt bearing two gem-methyl groups on the three carbon atom bridge exhibited a higher stereoselectivity (P_m = 0.90) than (SB-**2b**)-

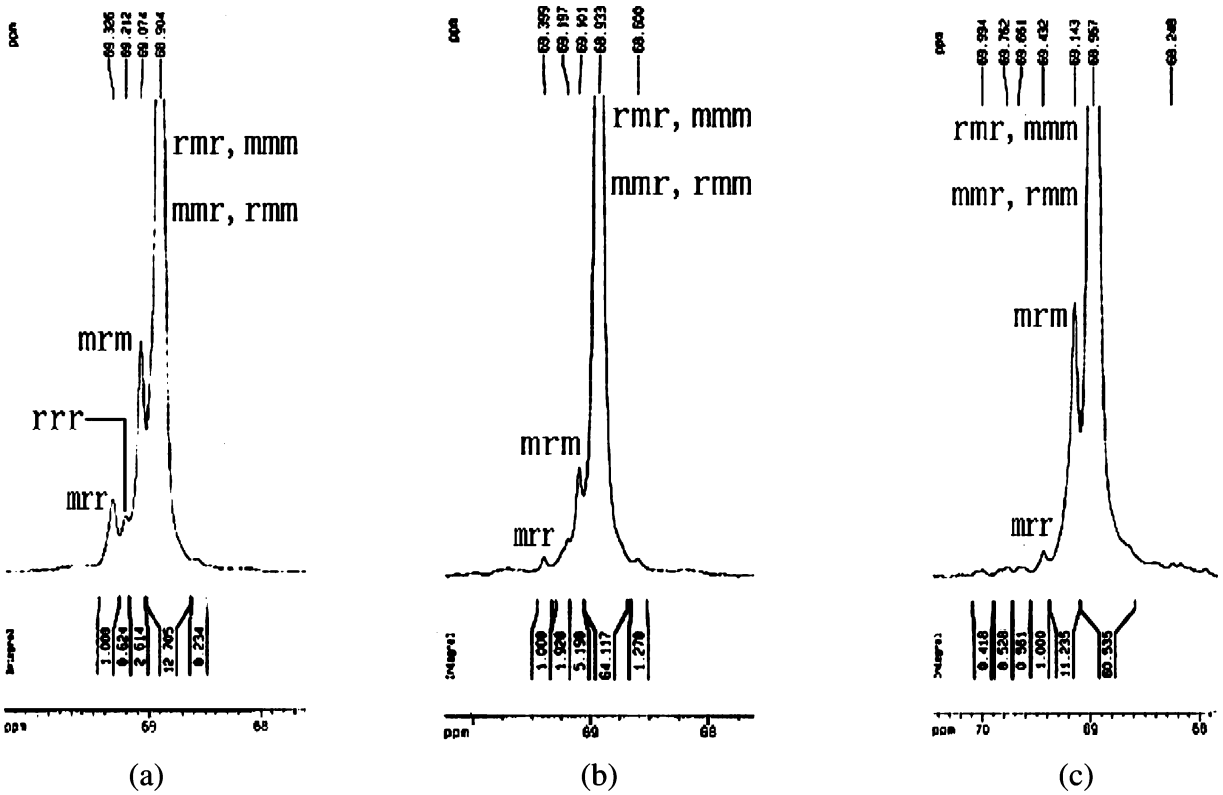

Figure 14. ^{13}C NMR spectra of poly(*rac*-LA) (methine region) prepared from (a) (SB-**1d**)AlEt, (b) (SB-**2d**)AlEt, and (c) (SB-**3b**)AlEt.

AlEt ($P_m = 0.86$) without gem-alkyl groups. Because of this uncertainty of the effect of backbone length and gem-alkyl groups on the backbone, it is difficult to conclude whether this deviation in stereoselectivity reflects a direct influence of the backbone nature or a competition between different initiating species resulting from the backbone nature.

To further investigate the relationship between the stereoselectivities of catalysts and their polymerization processes, ^{13}C NMR analyses of the methine region of poly(*rac*-LA) materials obtained from (SB-**1d**)AlEt, (SB-**2d**)AlEt, and (SB-**3b**)AlEt were conducted, and the spectra are shown in Figure 14. According to Bero et al.,[30] the existence of the *mrr* tetrad with chemical shift at ca. 69.4 ppm is the result of transesterification because the *mrr* tetrad is normally forbidden for pair-addition mechanism. The transesterification coefficient (*T*) was used to quantitative estimate the degree of transesterification, which was calculated by the ratio of I_{mrr}/I_{max}, where I_{mrr} is the intensity of the *mrr* tetrad and I_{max} is the maximal intensity in a completely transesterified poly(*rac*-LA). The calculated *T* values of (SB-**1d**)AlEt, (SB-**2d**)AlEt, and (SB-**3b**)AlEt are 47%, 11%, and 11%, respectively, and the *mrm* tetrad intensities of these materials prepared by (SB-**1d**)AlEt, (SB-**2d**)AlEt, and (SB-**3b**)-AlEt are 15.4%, 7.2%, and 15.4%. Considering that the *mrm* tetrad intensities of materials prepared by (SB-**1d**)AlEt and (SB-**3b**)AlEt are the same (ca. 15.4%), the decrease of stereoselectivity for (SB-**1d**)AlEt (67%) compared to (SB-**3b**)AlEt (71%) was largely attributed to the significant transeterification exhibited by a great *T* value of 47% for (SB-**1d**)AlEt. Moreover, the extents of transesterification caused by (SB-**2d**)AlEt and (SB-**3b**)AlEt were at the same level ($T = 11\%$), which suggested that the much higher stereoselectivity for (SB-**2d**)AlEt (90%) was mainly caused by the strong chain end control ability reflected by a relative low *mrm* tetrad intensity (7.2%) due to the steric bulky *tert*-butyl substituents.

Conclusions

In conclusion, we report a series of aluminum isopropoxides formed by in situ alcoholysis of ethyl complexes that act as single-site, living catalysts for the polymerization of *rac*-lactide. Structural analysis of these complexes reveals that although the aluminum ethyls are monomeric in both the solid and solution state, whether the aluminum isopropoxides can retain their monomeric properties in the solution largely relies on their substituents on the phenol rings. Microstructural analysis of the polymers formed by these complexes reveals that the tetradentate Schiff base ligands have the ability to control the tacticity of the growing polymer chains, and this ability varies according to different ligand surroundings. The bulky substituents on the Schiff base ligand influence the enantiomeric form of the lactide monomer incorporated next to the growing polymer chain and thus significantly influence the stereoselectivity. Furthermore, kinetic analysis suggests that, although polymerizations of *rac*-lactide by these complexes are first-order in lactide monomer, the active initiating species of them are distinguished and complex in the polymerization medium reflected by their noninteger orders in catalysts for the catalysts without steric hindered substituents. The bulky substituents protect the active species from being aggregated and slow down the polymerization rate. In contrast, electron-withdrawing substituents dramatically raise the polymerization rate without the diminishment of selectivity. In addition, the formation of a highly conjugated structure may also raise the polymerization rate and low the selectivity.

Acknowledgment. This project was financially supported by the National Natural Science Foundation of China (20574066), the National Fund for Distinguished Young Scholars (50425309), and the International Cooperation fund of Science and Technology (Key project 2005DFA50290).

Supporting Information Available: Experimental section, crystallographic data, and tables (Suppl. Table 1) giving full details of the crystal data. This material is available free of charge via the Internet at http://pubs.acs.org.

References and Notes

(1) (a) Chiellini, E.; Solaro, R. *Adv. Mater.* **1996**, *8*, 305−313. (b) Chabot, F.; Vert, M.; Chapelle, S.; Granger, P. *Polymer* **1983**, *24*, 53−59. (c) Uhrich, K. E.; Cannizzaro, S. M.; Langer, R. S.; Shakesheff, K. M. *Chem. Rev.* **1999**, *99*, 3181−3198. (d) Jeong, B.; Bae, Y. H.; Lee, D. S.; Kim, S. W. *Nature (London)* **1997**, *388*, 860−862.

(2) (a) Nijenhuis, A. J.; Grijpma, D. W.; Pennings, A. J. *Macromolecules* **1992**, *25*, 6419−6424. (b) Kowalski, A.; Libiszowski, J.; Duda, A.; Penczek, S. *Macromolecules* **2000**, *33*, 1964−1971. (c) Nimitsiriwat, N.; Marshall, E. L.; Gibson, V. C.; Elsegood, M. R. J.; Dale, S. H. *J. Am. Chem. Soc.* **2004**, *126*, 13598−13599. (d) Dove, A. P.; Gibson, V. C.; Marshall, E. L.; White, A. J. P.; Williams, D. J. *Chem. Commun.* **2001**, *3*, 283. (e) Aubrecht, K. B.; Hillmyer, M. A.; Tolamn, W. B. *Macromolecules* **2002**, *35*, 644−650.

(3) (a) Schwach, G.; Coudane, J.; Engel, R.; Vert, M. *Polym. Int.* **1999**, *46*, 177−182. (b) Nijenhuis, A. J.; Grijpma, D. W.; Pennings, A. J. *Macromolecules* **1992**, *25*, 6419−6424. (c) Coles, M. P.; Hitchcock, P. B. *Eur. J. Inorg. Chem.* **2004**, *13*, 2662−2672. (d) Chisholm, M. H.; Gallucci, J. C.; Zhen, H. *Inorg. Chem.* **2001**, *40*, 5051. (e) Chisholm, M. H.; Phomphrai, K. *Inorg. Chim. Acta* **2003**, *350*, 121−125. (f) Wu, J. C.; Huang, B. H.; Hsueh, M. L.; Lai, S. L.; Lin, C. C. *Polymer* **2005**, *46*, 9784−9792.

(4) (a) O'Keefe, B. J.; Monnier, S. M.; Hillmyer, M. A.; Tolman, W. B. *J. Am. Chem. Soc.* **2001**, *123*, 339−340. (b) McGuinness, D. S.; Marshall, E. L.; Gibson, V. C.; Steed, J. W. *J. Polym. Sci., Part A: Polym. Chem.* **2003**, *41*, 3798−3803. (c) Kricheldorf, H. R.; Serra, A. *Polym. Bull. (Berlin)* **1985**, *14*, 497−502. (d) Stolt, M.; Sodergard, A. *Macromolecules* **1999**, *32*, 6412−6417. (e) Wang, X.; Liao, K.; Quan, D.; Wu, Q. *Macromolecules* **2005**, *38*, 4611−4617. (f) Gibson, V. C.; Marshall, E. L.; Navarro-Llobet, D.; White, A. J. P.; Williams, D. J. *J. Chem. Soc., Dalton Trans.* **2002**, *23*, 4321−4322.

(5) (a) Chisholm, M. H.; Navarro-Llobet, D.; Simonsick, W. J., Jr. *Macromolecules* **2001**, *34*, 8851. (b) Chisholm, M. H.; Lin, C.-C.; Gallucci, J. C.; Ko, B.-T. *J. Chem. Soc., Dalton Trans.* **2003**, *3*, 406−412. (c) Huang, C.-H.; Wang, F.-C.; Ko, B.-T.; Yu, T.-L.; Lin, C.-C. *Macromolecules* **2001**, *34*, 356. (d) Kowalski, A.; Duda, A.; Penczek, S. *Macromolecules* **1998**, *31*, 2114−2122.

(6) (a) Chamberlain, B. M.; Sun, Y. P.; Hagadorn, J. R.; Hemmesch, E. W.; Young, V. G.; Pink, Jr., M.; Hillmyer, M. A.; Tolman, W. B. *Macromolecules* **1999**, *32*, 2400−2402. (b) Aubrecht, K. B.; Chang, K.; Hillmyer, M. A.; Tolman, W. B. *J. Polym. Sci., Part A: Polym. Chem.* **2001**, *39*, 284−293. (c) Spassky, N.; Simic, V.; Montaudo, M. S.; Hubert-Pfalzgraf, L. G. *Macromol. Chem. Phys.* **2000**, *201*, 2432−2440. (d) Chamberlain, B. M.; Jazdzewski, B. A.; Pink, M.; Hillmyer, M. A.; Tolman, W. B. *Macromolecules* **2000**, *33*, 3970−3977.

(7) (a) Kim, Y.; Jnaneshwara, G. K.; Verkade, J. G. *Inorg. Chem.* **2003**, *42*, 1437−1447. (b) Russell, S. K.; Gamble, C. L.; Gibbins, K. J.; Juhl, K. C. S.; Mitchell, W. S.; Tumas, A. J.; Hofmeister, G. E. *Macromolecules* **2005**, *38*, 10336−10340.

(8) For recent reviews on stereoselective polymerization of *rac*- or *meso*-lactide, see: (a) Dechy-Cabaret, O.; Martin-Vaca, B.; Bourissou, D. *Chem. Rev.* **2004**, *104*, 6147−6176. (b) O'Keefe, B. J.; Hillmyer, M. A.; Tolman, W. B. *J. Chem. Soc., Dalton Trans.* **2001**, 2215−2224. (c) Wu, J. C.; Yu, T.-L.; Chen, C.-T.; Lin, C.-C. *Coord. Chem. Rev.* **2006**, *250*, 602−626.

(9) Spassky, N.; Wisniewski, M.; Pluta, C.; LeBorgne, A. *Macromol. Chem. Phys.* **1996**, *197*, 2627−2637.

(10) (a) Ovitt, T. M.; Coates, G. W. *J. Am. Chem. Soc.* **2002**, *124*, 1316−1326. (b) Ovitt, T. M.; Coates, G. W. *J. Polym. Sci., Part A: Polym. Chem.* **2000**, *38*, 4686−4692.

(11) (a) Zhong, Z.; Dijkstra, P. J.; Feijen, J. *Angew. Chem.* **2002**, *114*, 4692−4695. (b) Zhong, Z.; Dijkstra, P. J.; Feijen, J. *J. Am. Chem. Soc.* **2003**, *125*, 11291−11298.

(12) (a) Nomura, N.; Ishii, R.; Akakura, M.; Aoi, K. J. *J. Am. Chem. Soc.* **2002**, *124*, 5938−5939. (b) Ishii, R.; Nomura, N.; Kondo, T. *Polym. J.* **2004**, *36*, 261−264.

(13) Tang, Z.; Chen, X.; Pang, X.; Yang, Y.; Zhang, X.; Jing, X. *Biomacromolecules* **2004**, *5*, 965−970.

(14) Duda et al. have succeeded in synthesizing stereoblock poly(*rac*-LA)s with T_m of 210 °C via the chiral ligand-exchange mechanism. For more information, see: Majerska, K.; Duda, A. *J. Am. Soc. Chem.* **2004**, *126*, 1026−1027.

(15) (a) The molecular structure of complex (SB-**2a**)AlEt will be presented in our next paper. (b) For the molecular structure of (SB-**2d**)AlEt, please see ref 13.

(16) Addison, A. W.; Rao, T. N.; Reedijk, J.; Van Rijin, J.; Verschoor, G. C. *J. Chem. Soc., Dalton Trans.* **1984**, *7*, 1349−1356.

(17) Atwood, D. A.; Harvey, M. J. *Chem. Rev.* **2001**, *101*, 37−52.

(18) For the molecular structure, stereoselectivity, and polymerization kinetics of catalyst (SB-**2d**)AlO^iPr, these detailed information are in: Tang, Z. H.; Chen, X. S.; Yang, Y. K.; Pang, X.; Sun, J. R.; Zhang, X. F.; Jing, X. B. *J. Polym. Sci., Part A: Polym. Chem.* **2004**, *42*, 5974−5982.

(19) Benn, R.; Rufinska, A.; Lemkuhl, H.; Janssen, E.; Kruger, C. *Angew. Chem., Int. Ed. Engl.* **1983**, *22*, 779−780.

(20) Such equilibrium between monomeric and dimeric initiating species of Schiff base aluminum catalysts have also been observed in ref 10a and Yang, J.; Yu, Y. H.; Li, Q. B.; Li, Y.; Cao, A. M. *J. Polym. Sci., Part A: Polym. Chem.* **2005**, *43*, 373−384.

(21) Dubois, P.; Jacobs, C.; Jerome, R.; Teyssie, P. *Macromolecules* **1991**, *24*, 2266−2270.

(22) According to present literature, the *p*-phenolate electron-withdrawing group either accelerates or retards the polymerization rate. For more information, see: (a) Cameron, P. A.; Jhurry, D.; Gibson, V. C.; White, Andrew. J. P.; Williams, D. J.; Williams, S. *Macromol. Rapid Commun.* **1999**, *20*, 616−618. (b) Bhaw-Luximon, A.; Jhurry, D.; Spassky, N. *J. Polym. Bull.* **2000**, *44*, 31−38. (c) Jhurry, D.; Bhaw-Luximon, A.; Spassky, N. *Macromol. Symp.* **2001**, *175*, 67−79. (d) Alcazar-Roman, L. M.; O'Keefe, B. J.; Hillmyer, M. A.; Tolman, W. B. *J. Chem. Soc., Dalton Trans.* **2003**, *15*, 3082−3087.

(23) (a) Williams, C. K.; Breyfogle, L. E.; Choi, S. K.; Nam, W.; Young, V. G., Jr.; Hillmyer, M. A.; Tolman, W. B. *J. Am. Chem. Soc.* **2003**, *125*, 11350−11359. (b) Chamberlain, B. M.; Cheng, M.; Moore, D. R.; Ovitt, T. M.; Lobkovsky, E. B.; Coates, G. W. *J. Am. Chem. Soc.* **2001**, *123*, 3229−3238. (c) O'Keefe, B. J.; Breyfogle, L. E.; Hillmyer, M. A.; Tolman, W. B. *J. Am. Chem. Soc.* **2002**, *124*, 4384−4393. (d) Kowalski, A.; Libiszowski, J.; Duda, A.; Penczek, S. *Macromolecules* **2000**, *33*, 1964−1971.

(24) Ropson, N.; Dubois, Ph.; Jerome, R.; Teyssie, Ph. *Macromolecules* **1995**, *28*, 7589−7598.

(25) Amgoune, A.; Thomas, C. M.; Roisnel, T.; Carpentier, J.-F. *Chem.−Eur. J.* **2006**, *12*, 169−179.

(26) (a) Thakur, K. A. M.; Kean, R. T.; Hall, E. S.; Kolstad, J. J.; Munson, E. J. *Macromolecules* **1998**, *31*, 1487−1494. (b) Thakur, K. A. M.; Kean, R. T.; Zell, M. T.; Padden, B. E.; Munson. E. J. *Chem. Commun.* **1998**, *17*, 1913−1914. (c) Chisholm, M. H.; Iyer, S. S.; Matison, M. E.; McCollum, D. G.; Pagel, M. *Chem. Commun.* **1997**, *20*, 1999−2000.

(27) (a) Wisniewski, M.; LeBorgne, A.; Spassky, N. *Macromol. Chem. Phys.* **1997**, *198*, 1227−1238. (b) Kasperczyk, J. E. *Macromolecules* **1996**, *28*, 3937−3939.

(28) Cai, C.-X.; Amgoune, A.; Lehmann, C. W.; Carpentier, J.-F. *Chem. Commun.* **2004**, *3*, 330−331.

(29) Hocking, P. J.; Marchessault, R. H. *Macromolecules* **1995**, *28*, 6401−6409.

(30) Bero, M.; Kasperczyk, J.; Jedlinski, Z. *Makromol. Chem.* **1990**, *191*, 2287−2296.

(31) Baran, J.; Duda, A.; Kowalski, A.; Szymanski, R.; Penczek, S. *Macromol. Rapid Commun.* **1997**, *18*, 325−333.

MA062194U